Journal of Vacuum Science and Technology A

RESEARCH ARTICLE | SEPTEMBER 22 2023

β-Ga_2O_3 orientation dependence of band offsets with SiO_2 and Al_2O_3

Special Collection: Gallium Oxide Materials and Devices

Hsiao-Hsuan Wan ; Jian-Sian Li ; Chao-Ching Chiang ; Xinyi Xia ; David C. Hays ; Fan Ren ; Stephen J. Pearton

J. Vac. Sci. Technol. A 41, 063205 (2023)
https://doi.org/10.1116/6.0003039

CrossMark

View Online

Export Citation

14 November 2023 23:52:13

AVS

JVST A
Journal of Vacuum Science & Technology A
ARTICLE
pubs.aip.org/avs/jva

β-Ga_2O_3 orientation dependence of band offsets with SiO_2 and Al_2O_3

Cite as: J. Vac. Sci. Technol. A **41**, 063205 (2023); doi: 10.1116/6.0003039
Submitted: 2 August 2023 · Accepted: 28 August 2023 ·
Published Online: 22 September 2023

View Online

Export Citation

CrossMark

Hsiao-Hsuan Wan,[1] Jian-Sian Li,[1] Chao-Ching Chiang,[1] Xinyi Xia,[1] David C. Hays,[2] Fan Ren,[1] and Stephen J. Pearton[3,a)]

AFFILIATIONS

[1]Department of Chemical Engineering, University of Florida, Gainesville, Florida 32611
[2]Nanoscale Research Facility, University of Florida, Gainesville, Florida 32611
[3]Department of Materials Science and Engineering, University of Florida, Gainesville, Florida 32611

Note: This paper is part of the Special Topic Collection on Gallium Oxide Materials and Devices.
[a)]**Author to whom correspondence should be addressed:** spear@mse.ufl.edu

ABSTRACT

Two of the most common dielectrics for β-Ga_2O_3 are SiO_2 and Al_2O_3 because of their large bandgaps, versatility of preparation, and thermal stability. However, because of the anisotropic properties of the β-polytype, it is necessary to understand differences in band alignment for the different crystal orientation. Using x-ray photoelectron spectroscopy, we performed a comparative study of the band alignment of SiO_2/β-Ga_2O_3 and Al_2O_3/ β-Ga_2O_3 heterojunctions with different β-Ga_2O_3 orientations of (001), (010), and ($\bar{2}$01). The bandgaps were determined to be 4.64, 4.71, and 4.59 eV for the ($\bar{2}$01), (001), and (010) oriented β-Ga_2O_3 substrates, respectively. The valence band offsets for SiO_2 on these three orientations were 1.4, 1.4, and 1.1 eV, respectively, while for Al_2O_3, the corresponding values were 0.0, 0.1, and 0.2 eV, respectively. The corresponding conduction band offsets ranged from 2.59 to 3.01 eV for SiO_2 and 2.26 to 2.51 eV for Al_2O_3.

Published under an exclusive license by the AVS. https://doi.org/10.1116/6.0003039

14 November 2023 23:52:13

I. INTRODUCTION

Ga_2O_3 is currently attracting interest for high power electronic devices with breakdown performance beyond the one-dimensional limits of both SiC and GaN.[1–12] The relatively low cost of manufacture makes these devices an option for kV class rectifiers for power converters in electric vehicles and their charging infrastructure.[1–5] Dielectrics are needed on β-Ga_2O_3 as gate insulators on transistors, edge termination structures on rectifiers, and surface passivation layers for encapsulation.[3–5] In most of these applications, there is a need to know the band alignment between the dielectric and the semiconductor to understand carrier accumulation and electric field profiles at the heterointerfaces. Two of the most common dielectrics for β-Ga_2O_3 are SiO_2 and Al_2O_3, which can be deposited by a range of techniques, including low damage atomic layer deposition, and selectively patterned with dry and wet etchants.[1,3,4] The band offset between SiO_2 and Al_2O_3 insulators in heterojunction conduction in Ga_2O_3 devices demonstrates its crucial significance, influencing the electronic transport characteristics and interfacial charge transfer dynamics at the junction interface. While several studies have reported the band alignments of these materials on β-Ga_2O_3 for specific crystallographic orientations,[13–18] there has not been a self-consistent examination of the band offsets for the three main commercially available substrate orientations.[17,19] Since the properties of β-Ga_2O_3 are anisotropic,[19–22] it is of value to establish the orientation dependence of band alignments. The use of the same cleaning procedure, deposition method, and thermal budget reduces variations in the measured valence band offsets.[23]

X-ray photoelectron spectroscopy was used to measure the valence band offsets of SiO_2 and Al_2O_3 on different β-Ga_2O_3 orientations of (001), (010), and ($\bar{2}$01) using the standard Kraut method.[24–26] The valence band offsets for SiO_2 on these three orientations were 1.4, 1.4, and 1.1 eV, respectively, while for Al_2O_3 the corresponding values were 0.0, 0.1, and 0.2 eV, respectively. Care was taken to minimize sample charging and other issues.[27] Conduction band offsets were derived from the directly measured valence band offsets and bandgaps of dielectrics and Ga_2O_3.[28]

Published under an exclusive license by the AVS

II. EXPERIMENT

Three β-Ga_2O_3 bulk substrates (10 × 15 mm) with different orientations, (001), (010), and ($\bar{2}01$), were purchased from NCT, Japan. All were nominally undoped, 0.65 mm thick, with n-type carrier concentrations of $<9 \times 10^{17}$ cm^{-3}. To indicate the crystal quality, the x-ray diffraction full width at half maximum in [100] and [010] azimuth directions was 50 arc sec in both cases. The root-mean-square surface roughness was <2 nm in all cases, as measured by atomic force microscopy of $10 \times 10\,\mu m^2$ areas. The front surface was chemically mechanically polished while the rear faces had ground finishes. The band alignments of atomic layer deposited (ALD) SiO_2 or Al_2O_3 on these substrates were measured after deposition conditions that have been described previously.[17,25,26] The layers for both dielectrics were deposited at 200 °C using tris (diethylamino) silane or trimethylaluminum as precursors, respectively, for SiO_2 or Al_2O_3. The temperature was chosen based on this being the optimum for insulator quality as judged by morphology and crystal quality. The layers are polycrystalline under these conditions.[17] For substrate cleaning predeposition, the following rinse sequence was employed: acetone, IPA, N_2 dry, and finally ozone exposure for 15 min. The ALD layers were deposited at 200 °C in a Cambridge Nano Fiji 200 using a remote inductively coupled plasma at 300 W to generate atomic oxygen. The bandgaps of the dielectrics were 8.7 eV for SiO_2 and 6.9 eV for Al_2O_3 as measured previously by reflection electron energy loss spectroscopy[29–31] and by the O1s peak from 200 nm dielectric reference layers.[25,26] 1.5 nm layers of SiO_2 or Al_2O_3 were deposited on the three Ga_2O_3 substrates in the same ALD deposition for measuring their core levels. This thickness is chosen so that the core levels in the underlying substrate can be measured through the insulator. The thicknesses were obtained from crystal balance calibrated measurements. The RMS roughness measured over $10 \times 10\,\mu m$ areas by atomic force microscopy was 1.8–2.1 nm for the 200 nm layers.

Valence band offsets were obtained from the Kraut method using XPS with a Physical Instruments ULVAC PHI system.[24] This uses an Al X-ray source with an energy of 1486.6 eV, a source power of 300 W, and an analysis area of 20 μm diameter. The standard take-off angle of 50° with an acceptance angle of ±7° was used for all spectra. For high resolution scans, the electron pass energy was 23.5 eV. The total energy resolution of the system is 0.5 eV, with an accuracy of 0.03 eV for the binding energies measured.

The procedure for determining the valence band offsets entails the determination of core level and valence band energy positions using three distinct Ga_2O_3 substrates along with 200 nm thick layers of dielectrics.[17,25–27] Subsequently, the subsequent phase involves the quantification of core level displacements within the SiO_2/Ga_2O_3 and Al_2O_3/Ga_2O_3 heterostructures. These displacements can be translated into their corresponding valence band offsets. Finally, the disparities in conduction band positions are inferred by leveraging the measured energy bandgaps and the valence band offsets.

III. RESULTS AND DISCUSSION

Figure 1 shows the determination of the bandgaps of the three different orientations of β-Ga_2O_3 from the onset of the plasmon

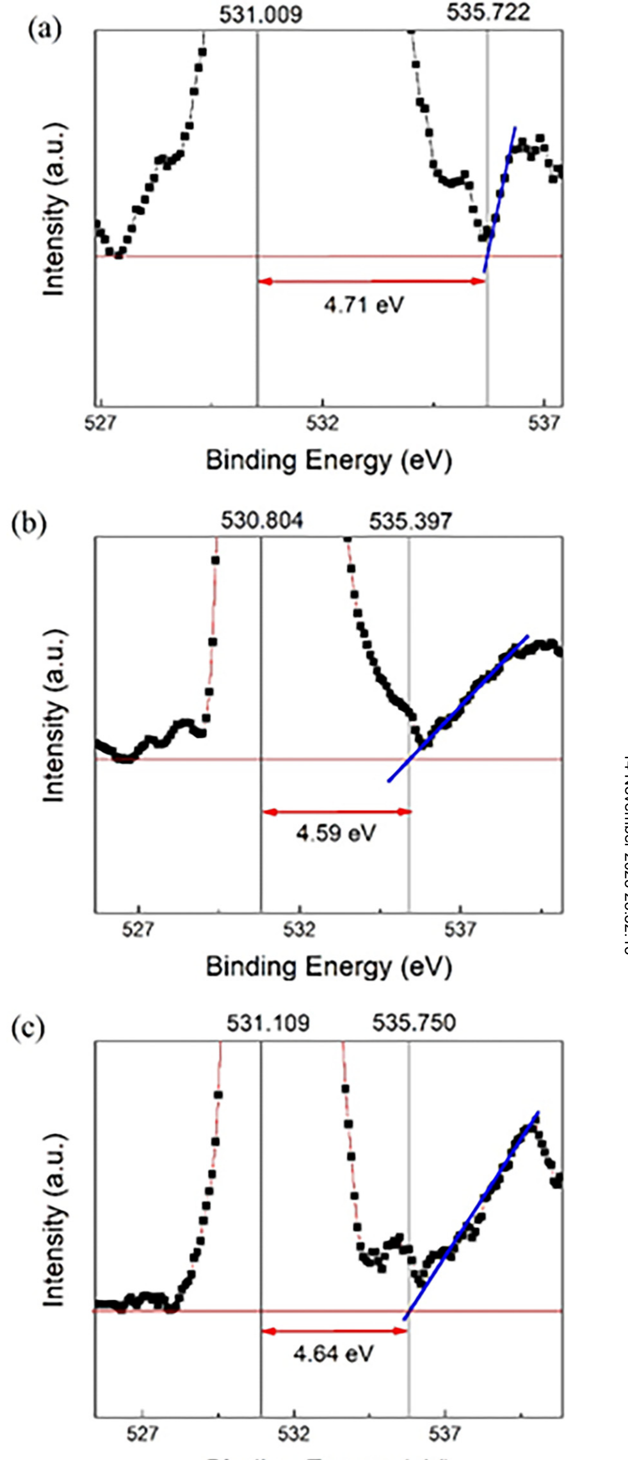

FIG. 1. Bandgap of (a) (001), (b) (010), and (c) ($\bar{2}01$) β-Ga_2O_3 determined using the onset of the plasmon loss feature in O 1s photoemission spectrum.

14 November 2023 23:52:13

Published under an exclusive license by the AVS

TABLE I. Valence band maximum and core level data used to calculate the bandgap of β-Ga_2O_3, SiO_2, and Al_2O_3.

Orientation	VBM	Core level peak (Ga 2p3)	Core-VBM	Bandgap
001	3.40	1118.1	1114.7	4.71 eV
010	3.40	1118.0	1114.6	4.59 eV
$\bar{2}01$	3.57	1118.2	1114.6	4.64 eV
	VBM	Core level peak	Core-VBM	Bandgap
SiO_2	5.7	104.3 (Si 2p)	98.6	8.7 eV
Al_2O_3	1.1	72.3 (Al 2p)	71.2	6.9 eV

loss feature in the O 1s photoemission spectra. Table I shows the valence band maxima and core level data used to calculate the bandgaps of Ga_2O_3. The bandgaps were determined to be 4.64, 4.71, and 4.59 eV for the ($\bar{2}01$), (001), and (010) oriented β-Ga_2O_3 substrates, respectively. These correspond closely to the previously reported values of 4.67, 4.72, and 4.57 eV for ($\bar{2}01$), (001), and (010) oriented β-Ga_2O_3 substrates, respectively, as determined from Tauc plots of the transmittance spectra.[17] Table I also shows the same data for the thick SiO_2 and Al_2O_3 layers, showing respective bandgaps of 8.7 and 6.9 eV. These are also consistent with previous reports.[17]

Figure 2 shows the delta core level energies for interfaces of thin SiO_2/β-Ga_2O_3 with orientation (a) (001), (b) (010), and (c) ($\bar{2}01$) from the differences in Ga 2p3 and Si 2p transitions. These are tabulated in the top of Table II for the SiO_2/β-Ga_2O_3 heterojunctions.

These data lead to the band alignment results of Fig. 3 for the SiO_2/β-Ga_2O_3 structures for the three different orientations of Ga_2O_3. All of the band alignments are type I, nested gap. The valence band offsets are, respectively, 1.4, 1.4, and 1.1 eV, for the (001), (010), and ($\bar{2}01$) orientations. This is consistent with a value of 1 eV reported by Konishi *et al.*[14] for plasma enhanced chemically vapor deposited SiO_2. The corresponding conduction band offsets are then 2.59, 3.01, and 2.66 eV for the (001), (010), and ($\bar{2}01$) orientations. Clearly, SiO_2 is an appropriate choice as a dielectric for β-Ga_2O_3 of any orientation in any of the possible applications noted earlier, since both the valence and conduction band offsets are larger than the commonly quoted rule of thumb of >1 eV.[28]

The data for delta core level energies for the Al_2O_3/β-Ga_2O_3 heterostructures are shown in Fig. 4 for (a) (001), (b) (010), and (c) ($\bar{2}01$) orientations of β-Ga_2O_3 from the differences in Ga 2p3 and Al 2p transitions. The data are also tabulated at the bottom of Table II.

The corresponding band alignment diagrams are shown in Fig. 5 for the Al_2O_3/ β-Ga_2O_3 structures. The valence band offsets are very small, being 0.1, 0.2, and 0.0 eV, respectively, for the (001), (010), and ($\bar{2}01$) orientations. These would not provide significant confinement of holes in device structures, although Al_2O_3 could still be used as passivation of field plate layers. The result for the ($\bar{2}01$) orientation is consistent with the previously reported value of 0.07 eV by Carey *et al.*[15,18] The corresponding conduction band offsets are 2.29, 2.51, and 2.26 eV for the (001), (010), and ($\bar{2}01$) orientations.

(a)

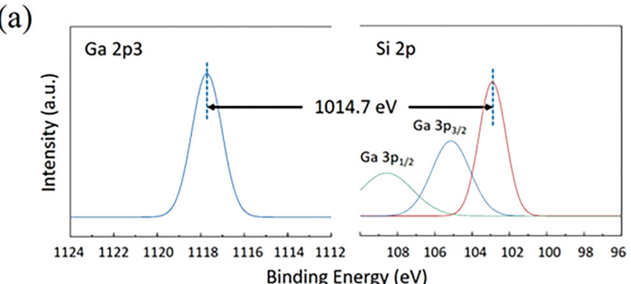

(b)

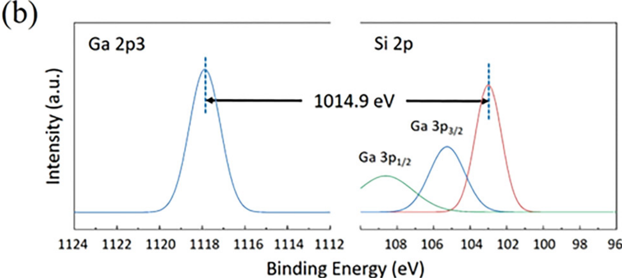

(c)

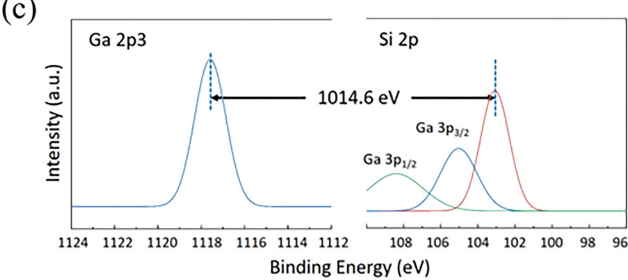

FIG. 2. Δ Core level energies for interfaces of thin SiO_2/β-Ga_2O_3 with orientation (a) (001), (b) (010), and (c) ($\bar{2}01$).

TABLE II. Core level data measured by XPS for SiO_2/β-Ga_2O_3 and Al_2O_3/β-Ga_2O_3.

Orientation	Core level peak (Ga 2p3)	Core level peak (Si 2p)	ΔCore level	ΔE_V	ΔE_C
001	1117.7	103.0	1014.7	1.4	2.59
010	1118.0	103.1	1014.9	1.1	3.01
$\bar{2}01$	1117.8	103.2	1014.6	1.4	2.66
Orientation	Core level peak (Ga 2p3)	Core level peak (Al 2p)	Core level	ΔE_V	ΔE_C
001	1117.9	74.3	1043.6	0.1	2.29
010	1118.0	74.4	1043.6	0.2	2.51
$\bar{2}01$	1117.7	74.3	1043.4	0.0	2.26

14 November 2023 23:52:13

Published under an exclusive license by the AVS

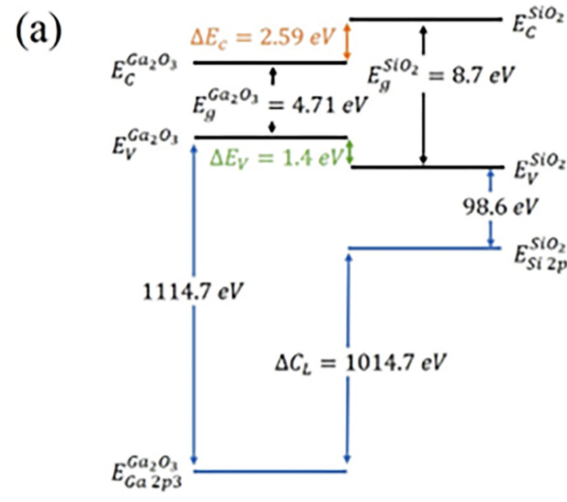

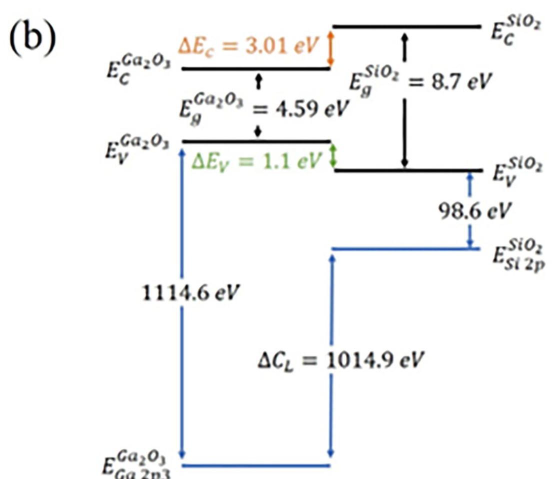

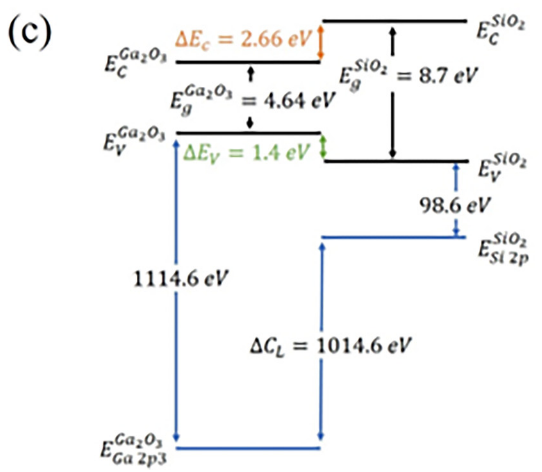

FIG. 3. Schematic of band alignments for SiO_2/β-Ga_2O_3 with orientation (a) (001), (b) (010), and (c) ($\bar{2}01$).

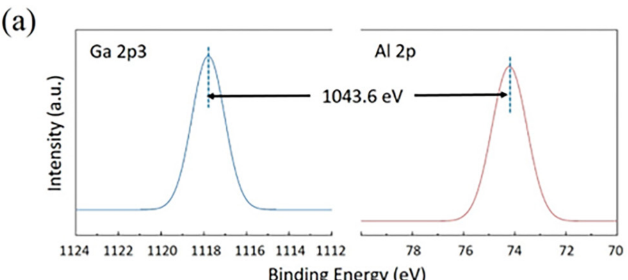

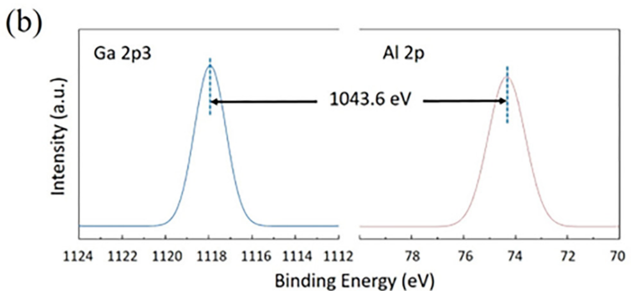

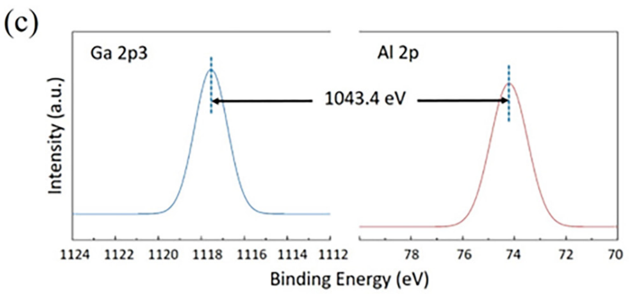

FIG. 4. Δ Core level energies for interfaces of thin Al_2O_3/β-Ga_2O_3 with orientation (a) (001), (b) (010), and (c) ($\bar{2}01$).

IV. SUMMARY AND CONCLUSIONS

We determined the band alignments for two common dielectrics on Ga_2O_3 for three orientations of this semiconductor. The dielectrics were deposited by low damage ALD, to avoid the type of interfacial disorder that is present during physical vapor depiction methods. The conduction band offsets in both SiO_2/β-Ga_2O_3 and Al_2O_3/β-Ga_2O_3 heterostructures are large and provide excellent electron confinement for all three major crystal orientations of β-Ga_2O_3, but the valence band offsets in the latter system are smaller than desirable for limiting hole transport. The differences in band alignment are relatively small for the different orientations, even though the properties of monoclinic β-Ga_2O_3 are anisotropic because of the low crystal symmetry. SiO_2 is a superior choice because of its larger valence band offsets, although Al_2O_3 could still have utility for surface passivation, field management, and encapsulation purposes.

14 November 2023 23:52:13

Published under an exclusive license by the AVS

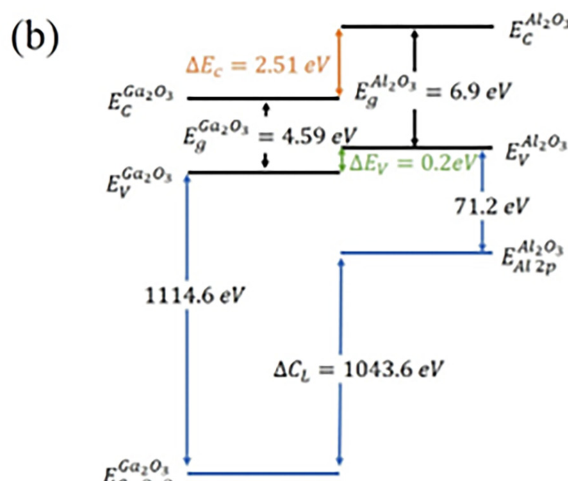

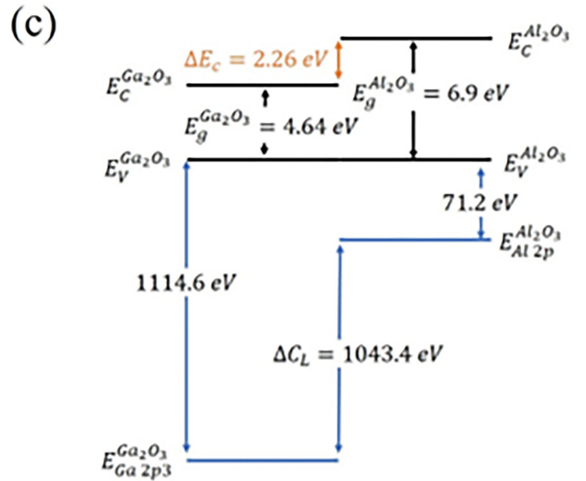

FIG. 5. Schematic of band alignments for Al_2O_3/ β-Ga_2O_3 with orientation (a) (001), (b) (010), and (c) ($\bar{2}01$).

ACKNOWLEDGMENTS

Work was performed as part of Interaction of Ionizing Radiation with Matter University Research Alliance (IIRM-URA), sponsored by the Department of the Defense, Defense Threat Reduction Agency under Award No. HDTRA1-20-2-0002. The content of the information does not necessarily reflect the position or the policy of the federal government, and no official endorsement should be inferred. The authors thank the staff of the Nanoscale Research Facility at UF, part of the Herbert Wertheim College of Engineering's Research Service Center (RSC), for assistance in device fabrication.

AUTHOR DECLARATIONS

Conflict of Interest

The authors have no conflicts to disclose.

Author Contributions

Hsiao-Hsuan Wan: Conceptualization (equal); Data curation (equal); Formal analysis (equal); Funding acquisition (equal); Investigation (equal); Methodology (equal); Software (equal); Validation (equal); Visualization (equal); Writing – original draft (equal); Writing – review & editing (equal). **Jian-Sian Li:** Formal analysis (equal); Investigation (equal); Methodology (equal). **Chao-Ching Chiang:** Data curation (equal); Formal analysis (equal); Methodology (equal). **Xinyi Xia:** Data curation (equal); Formal analysis (equal); Investigation (equal); Methodology (equal). **David C. Hays:** Data curation (equal); Formal analysis (equal); Investigation (equal); Methodology (equal). **Fan Ren:** Conceptualization (equal); Funding acquisition (equal); Methodology (equal); Project administration (equal); Resources (equal); Supervision (equal); Writing – original draft (equal); Writing – review & editing (equal). **Stephen J. Pearton:** Conceptualization (equal); Project administration (equal); Supervision (equal); Writing – original draft (equal); Writing – review & editing (equal).

14 November 2023 23:52:13

DATA AVAILABILITY

The data that support the findings of this study are available within the article.

REFERENCES

[1]S. J. Pearton, J. Yang, P. H. Cary, F. Ren, J. Kim, M. J. Tadjer, and M. A. Mastro, Appl. Phys. Rev. **5**, 011301 (2018).
[2]M. H. Wong and M. Higashiwaki, IEEE Trans. Electron Devices **67**, 3925 (2020).
[3]A. J. Green *et al.*, APL Mater. **10**, 029201 (2022).
[4]S. J. Pearton, F. Ren, M. Tadjer, and J. Kim, J. Appl. Phys. **124**, 220901 (2018).
[5]P. P. Sundaram, F. Alema, A. Osinsky, and Steven J. Koester, J. Vac. Sci. Technol. A **40**, 043211 (2022).
[6]C. Wang *et al.*, J. Phys. D: Appl. Phys. **54**, 243001 (2021).
[7]K. Kaneko, K. Uno, R. Jinno, and S. Fujitsu, J. Appl. Phys. **131**, 090902 (2022).
[8]J. Zhang *et al.*, Nat. Commun. **13**, 3900 (2022).
[9]K. D. Chabak *et al.*, Semicond. Sci. Technol. **35**, 013002 (2020).
[10]C. Liao *et al.*, IEEE Trans. Electron Devices **69**, 5722 (2022).
[11]Y. Wang *et al.*, IEEE Trans. Power Electron. **37**, 3743 (2022).

Published under an exclusive license by the AVS

[12]H. Gong *et al.*, IEEE Trans. Power Electron. **36**, 12213 (2021).
[13]P. P. Sundaram, F. Liu, F. Alema, A. Osinsky, B. Jalan, and S. J. Koester, Appl. Phys. Lett. **122**, 232105 (2023).
[14]K. Konishi, T. Kamimura, M. H. Wong, K. Sasaki, A. Kuramata, S. Yamakoshi, and M. Higashiwaki, Phys. Status Solidi B **253**, 623 (2016).
[15]P. H. Carey, F. Ren, D. C. Hays, B. P. Gila, S. J. Pearton, S. Jang, and A. Kuramata, Vacuum **142**, 52 (2017).
[16]M. Hattori *et al.*, Jpn. J. Appl. Phys. **55**, 1202B6 (2016).
[17]C. Fares, F. Ren, M. Kneiß, H. Wenckstern, M. Grundmann, and S. J. Pearton, *Wide Bandgap Semiconductor-Based Electronics*, edited by F. Ren and S. J. Pearton (IOP, Bristol, 2020).
[18]P. H. Carey, F. Ren, D. Hays, B. P. Gila, and S. J. Pearton, *Metal Oxides, Gallium Oxide*, edited by S. J. Pearton, F. Ren, and M. Mastro (Elsevier, Oxford, 2019), Chap. 13, pp. 287–311.
[19]Y. Deng *et al.*, Appl. Surf. Sci. **622**, 156917 (2023).
[20]Z. Guo *et al.*, Appl. Phys. Lett. **106**, 111909 (2015).
[21]R. Yatskiv, S. Tiagulskyi, and J. Grym, J. Electron. Mater. **49**, 5133 (2020).
[22]W. Mu, X. Chen, G. He, Z. Jia, J. Ye, B. Fu, J. Zhang, S. Ding, and X. Tao, Appl. Surf. Sci. **527**, 146648 (2020).
[23]C. Fares, F. Ren, D. C. Hays, B. P. Gila, and S. J. Pearton, ECS J. Solid State Sci. Technol. **8**, Q3001 (2019).
[24]E. A. Kraut, R. W. Grant, J. R. Waldrop, and S. P. Kowalczyk, Phys. Rev. Lett. **44**, 1620 (1980).
[25]D. C. Hays, B. P. Gila, S. J. Pearton, and F. Ren, Appl. Phys. Rev. **4**, 021301 (2017).
[26]C. Fares, F. Ren, E. Lambers, D. C. Hays, B. P. Gila, and S. J. Pearton, J. Vac. Sci. Technol., B **36**, 061207 (2018).
[27]G. H. Major, V. Fernandez, N. Fairley, E. F. Smith, and M. R. Linford, J. Vac. Technol., A **40**, 063201 (2022).
[28]J. Robertson, J. Vac. Sci. Technol., B **18**, 1785 (2000).
[29]Z. L. Wang and J. M. Cowley, Surf. Sci. **193**, 501 (1988).
[30]M. Vos, J. Electron Spectrosc. Relat. Phenom. **191**, 65 (2013).
[31]M. Vos, S. W. King, and B. L. French, J. Electron Spectrosc. Relat. Phenom. **212**, 74 (2016).

14 November 2023 23:52:13

Published under an exclusive license by the AVS